

# Attention to Neural Plagiarism: Diffusion Models Can Plagiarize Your Copyrighted Images!

Zihang Zou<sup>1</sup> Boqing Gong<sup>2</sup> Liqiang Wang<sup>1</sup>

<sup>1</sup>University of Central Florida

<sup>2</sup>Boston University

{zihang.zou, liqiang.wang}@ucf.edu, bgong@bu.edu

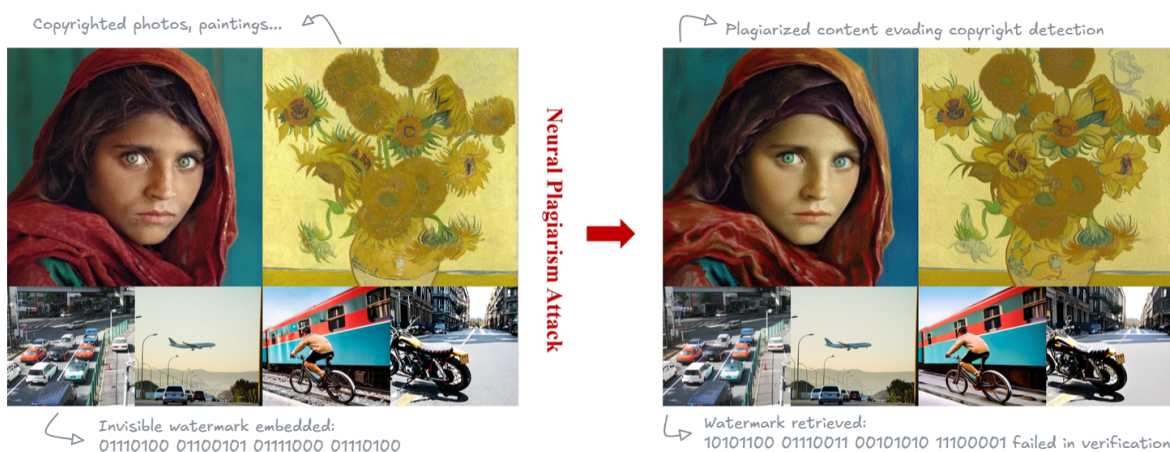


Figure 1. Copyrighted images (top left) and watermarked data (bottom left) can be easily plagiarized by diffusion models.

## Abstract

In this paper, we highlight a critical threat posed by emerging neural models—data plagiarism. We demonstrate how modern neural models (e.g., diffusion models) can effortlessly replicate copyrighted images, even when protected by advanced watermarking techniques. To expose the vulnerability in copyright protection and facilitate future research, we propose a general approach regarding neural plagiarism that can either forge replicas of copyrighted data or introduce copyright ambiguity. Our method, based on “anchors and shims”, employs inverse latents as anchors and finds shim perturbations that can gradually deviate the anchor latents, thereby evading watermark or copyright detection. By applying perturbation to the cross-attention mechanism at different timesteps, our approach induces varying degrees of semantic modifications in copyrighted images, making it to bypass protections ranging from visible trademarks, signatures to invisible watermarks. Notably, our method is a purely gradient-based search that requires no additional training or fine-tuning. Empirical experiments on MS-COCO and real-world copyrighted im-

ages show that diffusion models can replicate copyrighted images, underscoring the urgent need for countermeasures against neural plagiarism. Source code is available at: <https://github.com/zzzucf/Neural-Plagiarism>.

## 1. Introduction

Plagiarism has long been a critical concern for data copyrights, and recent advances in generative models [36, 37, 39, 42, 57] have intensified this issue. These neural generative models, trained on vast datasets, are capable of producing high quality images, showing a troubling potential for what we term “neural plagiarism”. Specifically, they may memorize training data and then directly reproduce copyrighted content [5, 7], or generate outputs that closely resemble copyrighted works. As generative AI continues to evolve, the risk of copyright infringement escalates across a broad spectrum of data types, including watermarked user’s data, photographs, artworks, signatures, and human portraits.

Legal regulations have been put in place to counteract the misconducts of neural models. For example, the Gen-

eral Data Protection Regulation (GDPR) [2] prohibits neural models to train on user’s data without consent; traditional copyright laws [1] and trademark laws [48] restrict generative AI from producing copyrighted images.

Beyond legal measures, technical approaches have also been implemented to protect intellectual property. Watermarking has proven to be an effective tool for copyright protection [17, 56], particularly in digital media. Visual watermarks, such as trademarks and signatures, are widely used to assert ownership and deter unauthorized use of images. Additionally, emerging invisible watermarking techniques [17, 56, 60] enable content creators to embed robust copyright protections within digital assets without noticeably degrading image quality.

Despite these legal frameworks and technical efforts, diffusion models show a great potential to plagiarism as it can effortlessly generate replicas [3, 28, 59] of copyrighted data while circumventing protection measures like watermarking [3, 22, 27, 59].

In this work, we focus on plagiarism of copyrighted images from diffusion models. We propose a novel “shim” and “anchor” method for diffusion models to enable optimization in latent space where we can gradually modify semantic information to bypass copyright protections. We also present a novel perturbation technique based on attention, where we aim to find the alternative query, key and value that generate outputs as original ones to maintain the semantic consistency.

In summary, our main contributions are as follow:

- Introduce a general neural plagiarism pipeline for diffusion models that exposes vulnerabilities in existing data copyright protection methods and hence facilitate the development of more effective copyright protections.
- Develop a controllable search-based method and introduce a novel attention-based perturbation technique for diffusion models that enables a coarse-to-fine exploration of the semantic space with low memory consumption.
- Present a comprehensive analysis of forgery and ambiguity attacks that can lead to plagiarism in real-world cases, ranging from copyrighted artworks, signature, trademark to invisible watermarked data.

## 2. Related Work

### Intellectual Property and Traditional Watermarking.

Intellectual property (IP) is fundamental to human society—it incentivizes creativity, rewards innovation, and preserves culture. For example, Disney’s IP, such as Mickey Mouse, The Lion King, Frozen, is strictly protected under copyright laws [48] to prevent unauthorized use and plagiarism. Beyond legal protections, watermarking has long been an effective method for securing copyrighted content. Traditional techniques achieve this by embedding watermarks through geometric transformations in the frequency

domain [17, 30]. These techniques create invisible watermark yet remain vulnerable to image distortions.

With recent development in artificial intelligence, deep learning models have emerged for robust watermark embedding. HiDDeN [60] introduces an encoder–decoder framework while leveraging adversarial training [16] to improve watermark resilience. Subsequent studies explore self-supervised learning [56] to embed watermarks in latent spaces, employ attention mechanisms [12], and utilize differentiable simulations of real-world distortions [46] to further enhance robustness of watermarking.

### Copyright Protection and Threats from Generative AI.

Recent advancements in diffusion models [20, 34, 39, 43, 44] have ushered in a new era of generative AI, enabling the creation of highly realistic images, videos, and sounds that are virtually indistinguishable from reality. However, these breakthroughs have also raised concerns over misuse, such as deepfakes [14, 45, 47]. In response, legal frameworks now require AI-generated content to be clearly labeled with a visible watermark.

To comply with legal requirements and protect copyrights, researchers are developing watermarking techniques specific to generative models, in particular, diffusion models. For instance, Stable Signature [13] fine-tunes a VAE decoder to embed watermarks within images, which can then be extracted using a pretrained message decoder from HiDDeN [60]. In comparison to traditional invisible watermark methods, Tree-Rings Watermark approach [52] injects a tree-ring-like watermark into the Fourier frequency domain of latent variables, generating semantically similar content while ensuring the latent watermark remains resilient to common image distortions. Building on this idea, Gaussian Shading [53] employs a quantile-based method to mitigate the significant distribution shift in latent variables caused by the tree-ring watermark, achieving performance-lossless watermarking. Moreover, RingID [9] enhances the tree-ring approach with greater precision by incorporating multi-key identification through a series of augmented transformations.

Like a double-edged sword, these generative models unfortunately show greater potential for infringing copyrighted data. **Forgery attacks or regeneration attacks**, compromise data ownership by removing original watermarks [22, 26, 27, 41, 59], making it difficult to trace content back to its source. In particular, Regen [59] exploits diffusion models by adding noise in the forward process for a few step and then denoising via the reverse process, effectively removing most invisible watermarks [13, 17, 56]. Rinse [3] iterates this process multiple times to further improve watermark removal. Additionally, recent work [27] leverages ControlNet [57] and extra image encoder [33] to regenerate the watermarked images from clean noise under semantic constraints, thus removing latent watermarks like

Tree-ring [52].

Finally, **ambiguity attacks** [54] remain an underestimated threat to copyright protection. In these attacks, replicas are generated with alternative watermarks linked to different “original data”, creating competing claims of ownership and complicating the verification of the rightful owner. Despite their significant risks, existing defenses are limited, with the few available methods addressing only very specific scenarios [11, 55]. The only practical defense based on data creation timestamps is largely inapplicable, as creation times are often unrecorded in real-world cases.

### 3. The Rising Threat —“Neural Plagiarism”

In this work, we focus on posing a new threat, denoted as neural plagiarism, which exploits neural models to *replicate copyrighted data*, while confusing or evading existing copyright protection method. In this section, we formalize this problem into a scenario involved with a data owner, an attacker and a third-party verifier.

**Scope of Copyrighted Data.** We primarily focus on image data and address a broad range of data types subject to copyright protection in real-world scenarios. This includes traditional forms of copyrighted data, such as photographs, paintings, artworks and trademarks, as explicitly defined by copyright laws [1, 48]. Additionally, we consider user owned data protected by watermarking techniques.

**Data Owner’s Capabilities.** Given an image data  $x$ , a data owner can choose the watermarking method along with watermark  $w$  (e.g., a hidden bit stream [46, 60], a registered trademark or simply copyrighted images) and publishes only watermarked data  $x^w$ .

**Attacker’s Ability.** An attacker only has access to the copyrighted data  $x^w$  without knowing the watermark.

**The Plagiarism Attacks.** Formally, an attacker aims to develop a generative model  $\mathcal{G}$  that replicates copyrighted data  $x^w$ , protected by a watermark  $w$ . The plagiarism occurs when the distance between the replicated  $x^*$  and  $x^w$  is small,

$$x^* = \mathcal{G}(x^w) \text{ s.t. } d(x^*, x^w) < \delta \quad (1)$$

Here,  $d$  is a distance function (e.g.,  $l_2$  distance, perceptual distance [58] or human justifications) and  $\delta$  is a predefined threshold.

Given a third-party verifier  $\mathcal{V}$ , who can arbitrate the data ownership by recovering the watermark  $w$  (e.g. comparing bit accuracy, watermark pattern or copyrights violation), two major types of plagiarism attacks are considered:

- **Forgery Attack:** An adversary leverages a generative model to replicate the copyrighted image while effectively removing the embedded watermark, which leads to a verification failure  $\mathcal{V}(x^*) \neq w$ .
- **Ambiguity Attack:** This attack removes the original watermark and creates ownership ambiguity by embedding

an alternative watermark, causing problem in copyright arbitration:  $\mathcal{V}(x^*) = w^*$  and  $\mathcal{V}(x^w) = w$  while  $x^*$  and  $x^w$  are visually similar.

## 4. Towards Neural Plagiarism Attacks

Without loss of generality, this paper focuses on copyrighted images, including real-world copyrighted images and AI-generated images from diffusion models.

### 4.1. Background

Diffusion models [20, 34, 39, 43, 44], originally inspired by thermodynamics, operate as denoising auto-encoders that iteratively remove noise from an image. In the **forward process**, noise is gradually injected into an initial image  $\mathbf{x}_0$ , eventually transforming it into an isotropic Gaussian. This process is defined as

$$q(\mathbf{x}_{1:T}|\mathbf{x}_0) = \prod_{t=1}^T q(\mathbf{x}_t|\mathbf{x}_{t-1}),$$

where  $q(\mathbf{x}_t|\mathbf{x}_{t-1}) = \mathcal{N}(\mathbf{x}_t; \sqrt{1-\beta_t}\mathbf{x}_{t-1}, \beta_t\mathbf{I})$  for each timestep. Using the reparameterization trick [24], the noisy image at step  $t$  can be expressed as

$$\mathbf{x}_t = \sqrt{\alpha_t}\mathbf{x}_0 + \sqrt{1-\alpha_t}\epsilon \quad (2)$$

The **reverse (denoising) process** aims to recover the original image by progressively removing the injected noise. It is modeled as

$$p_\theta(\mathbf{x}_{0:T}) = p(\mathbf{x}_T) \prod_{t=1}^T p_\theta(\mathbf{x}_{t-1}|\mathbf{x}_t),$$

with  $p_\theta(\mathbf{x}_{t-1}|\mathbf{x}_t) = \mathcal{N}(\mathbf{x}_{t-1}; \boldsymbol{\mu}_\theta(\mathbf{x}_t, t), \boldsymbol{\Sigma}_\theta(\mathbf{x}_t, t))$ .

In this formulation, the network learns to predict the mean  $\boldsymbol{\mu}_\theta(\mathbf{x}_t, t)$  and covariance  $\boldsymbol{\Sigma}_\theta(\mathbf{x}_t, t)$  that effectively reverse the forward diffusion. Recent advances, such as deterministic solvers [29], enable the **inversion process** [21, 29, 50] by iteratively reversing the deterministic reverse process, targeting the original latent variable that generates the image  $x$ .

In practice, the reverse process is facilitated by a neural network based on the UNet architecture [40], denoted as  $\epsilon_\theta$ . This network is tasked with predicting the noise  $\epsilon$  added at each diffusion step. Given a noisy image  $\mathbf{x}_t$  and the corresponding timestep  $t$ ,  $\epsilon_\theta(\mathbf{x}_t, t)$  estimates the noise component, which is used to guide the denoising process. The network is trained by minimizing the mean squared error between the true noise and the predicted noise:

$$\mathcal{L}_{\text{simple}} = \mathbb{E}_{t, \mathbf{x}_0, \epsilon} \left[ \|\epsilon - \epsilon_\theta(\sqrt{\alpha_t}\mathbf{x}_0 + \sqrt{1-\alpha_t}\epsilon, t)\|^2 \right].$$

As a result, diffusion models are well-suited for data plagiarism. They can regenerate images through the inverse and denoising process [59] and enable further optimization of semantic content via latent variables.

## 4.2. Intuitive Objective Function

The plagiarism attack aims to replicate a target copyrighted image  $\mathbf{x}_0^w$  by generating a visually similar attack output  $\mathbf{x}_0^*$ . In diffusion models, latent variables at different timesteps capture various features and may contain embedded watermarks (e.g., Tree-Ring [52] injects watermark on latent variables). Therefore, it is intuitive to modify the latent representation. By increasing the distance between the latent representations of the copyrighted and attack images, the embedded watermark is likely to be disrupted or removed. Formally, we construct our intuitive objective function as:

$$\min_{\mathbf{x}_T^*} d_{\text{visual}}(\mathbf{x}_0^w, \mathbf{x}_0^*) - \gamma d_{\text{latent}}(\mathbf{x}_T, \mathbf{x}_T^*) \quad (3)$$

where  $\gamma$  is a hyperparameter,  $d_{\text{visual}}$  and  $d_{\text{latent}}$  are distance metrics designed to maintain image similarity while encouraging differences in the latent space.

However, through preliminary experiments (see Appendix for more details), we found that this simple objective is difficult to achieve based on the following challenges:

- **High Memory Consumption:** Optimizing Eq. 3 requires computing  $\frac{\partial \mathbf{x}_{t-1}^*}{\partial \mathbf{x}_t^*}$  at every timestep, consuming roughly 10 GB of GPU memory per step. Even a DPM solver [29] with only 10 steps would demand over 100 GB, which far exceeds the memory limits of most GPUs.
- **Over-smoothing Images:** To reduce memory usage, some researchers estimate gradients by skipping several sampling steps [51]. However, this shortcut tends to over-smooth images.
- **Noisy Outputs:** High perturbation in the latent space often results in noisy images rather than meaningful semantic alterations.

## 5. Method

To address above challenges, we propose an optimization framework using *anchors* and *shims*, as shown in Figure 2.

### 5.1. Optimization with Anchors and Shims

We first obtain **anchors** as a guideline for subsequent optimization. Given a target image  $x$  (i.e., a copyrighted image  $x^w$ ), we encode it into latent space via VAE encoder [38], obtaining the latent representation  $\hat{\mathbf{x}}_0$ . By inverting the generation process [18] of a deterministic solver (e.g., DPM [29]), we obtain a sequence of anchors as,

$$\{\hat{\mathbf{x}}\}_{i=1}^T := \{\hat{\mathbf{x}}_1, \dots, \hat{\mathbf{x}}_T\} \quad (4)$$

The above inverse latents can be used to generate semantically similar images. Here,  $\hat{\mathbf{x}}_T$  is often used for latent watermark retrieval [52, 53]. Our intuitive objective is to find a perturbed  $\mathbf{x}_T^*$  that is far away from  $\hat{\mathbf{x}}_T$  (see eq 3). However, since we only focus on replicating copyrighted image  $x$ , we

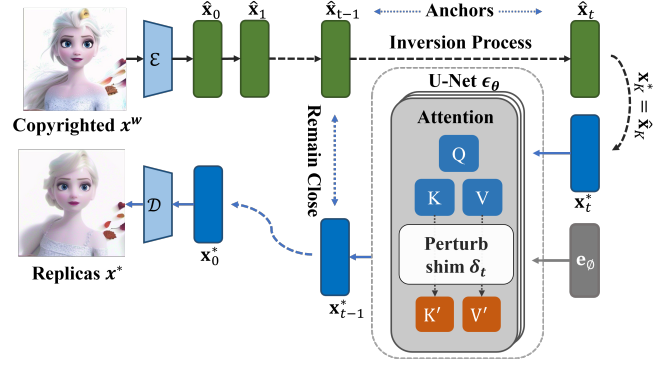


Figure 2. Attack pipeline overview for Neural plagiarism.

can relax this goal to allow perturbation at arbitrary timestep  $t$ , as long as the resulting  $\mathbf{x}_t^*$  yields satisfiable replication. Formally, we define this perturbation process as  $\Delta(\cdot)$  along with a margin variable  $\delta_t$ ,

$$\mathbf{x}_t^* = \Delta_{\delta_t \in \mathcal{S}}(\mathbf{x}_t, \delta_t) \quad (5)$$

Notably,  $\Delta$  is defined in a general form, indicating the perturbation could occur in any space  $\mathcal{S}$  - not necessarily restricted to the latent space. Instead to learn  $\mathbf{x}_t^*$  directly, we find  $\delta_t$ , referred as the **shim** during optimization. The norm of  $\delta_t$  is referred as *the least* distance between the input and its perturbed result in the perturbation space  $\mathcal{S}$ .

The term “anchors” and “shim” originate from the alignment process in door installation, where a handyman inserts wooden shims at various locations to adjust spacing, ensuring uniform gaps to the anchors. Inspired by this concept, we perturb latent by adjusting  $\delta_t$  with a loss term,

$$\mathcal{L}_{\text{norm}}(t) = \max(0, \hat{\varepsilon}_t - \|\delta_t\|) \quad (6)$$

Here, the  $\hat{\varepsilon}_t$  is the hyper-parameter to ensure a sufficient large distance.

By adding shims to the latent variables, the resulting representations are likely to diverge from the anchors, thereby disrupting embedded watermarks and removing copyrighted information.

### 5.2. Semantic Search via Attention Perturbation

We aim to extract the semantically equivalent information from diffusion models to form a semantic search space when forging replicas. In stable diffusion, a conditional image generator is implemented by the cross-attention mechanism [49] to align semantic prompts with images. By employing the UNet backbone and domain specific encoder  $\tau_\theta$ , the cross attention is implemented as  $\text{Attention}(Q, K, V) = \text{softmax}\left(\frac{QK^T}{\sqrt{d_k}}\right)V$  [38], where

$$Q = W_Q^{(i)} \varphi_i(z_t), \quad K = W_K^{(i)} \tau_\theta(y), \quad V = W_V^{(i)} \tau_\theta(y).$$

Here,  $W_Q^{(i)}$ ,  $W_K^{(i)}$ , and  $W_V^{(i)}$  are learnable projection matrices;  $\varphi_i(z_t)$  denotes a flattened intermediate representation of the U-Net implementing  $\epsilon_\theta$ ;  $\tau_\theta$  is the CLIP encoder [35] to map a prompt  $y$  into high-dimensional, dense text embeddings.

Our goal is to discover an alternative set of  $(Q', K', V')$  that yield similar outputs to the original ones. At each diffusion timestep  $t$ , we inject ‘‘shim’’  $\delta_t$  on the text embedding only. To preserve semantic consistency, we maximize cosine similarity,

$$\mathcal{L}_{\text{semantic}}(t) = -\frac{\mathbf{e}_\theta \cdot (\mathbf{e}_\theta + \delta_t)}{\|\mathbf{e}_\theta\| \|\mathbf{e}_\theta + \delta_t\|} \quad (7)$$

Here,  $\mathbf{e}_\theta$  denotes the text embedding of an empty string, as encoded by the CLIP text encoder. This is a standard setting for unconditional generation and inversion [32].

Meanwhile, to ensure the perturbed latents can produce similar outputs, we align the predicted next latent to remain close to its corresponding anchor,

$$\mathcal{L}_{\text{align}}(t) = d(\mathbf{x}_{t-1}, \hat{\mathbf{x}}_{t-1}) \quad (8)$$

Specifically, we perturb with  $\mathbf{x}_t^* = \Delta(\mathbf{x}_t, \delta_t)$  and remove the noise predicted by UNet:  $\mathbf{x}_{t-1} \leftarrow \mathbf{x}_t^* - \zeta_t \cdot \epsilon_\theta(\mathbf{x}_t^*, t)$  with coefficient  $\zeta_t$  specified by different solvers.

### 5.3. The Iterative Searching Process

Equations 6, 7, 8 together define our new objective: *insert a large enough shim to induce semantic changes while keeping outputs remain close to anchors*. At a timestep  $t$ ,  $\delta_t$  is being searched jointly by,

$$\min_{\delta_t} \mathcal{L}_{\text{norm}}(t) + \gamma_1 \mathcal{L}_{\text{semantic}}(t) + \gamma_2 \mathcal{L}_{\text{align}}(t) \quad (9)$$

with  $\gamma_1$  and  $\gamma_2$  be the hyper-parameters.

Keen readers may have realized the major reason to introduce anchors and shims is to alleviate the aforementioned memory consumption issue. As we preserve the trajectory as anchors, we decouple the chain of latents, thereby we are free to adjust the shims at arbitrary timesteps — one by one.

Besides, the perturbation process can be done only on selected timesteps, improving the efficiency significantly. Notably, we add shims at specific timesteps, indicating that the semantic search space evolves over time. In particular, as  $t$  decreases from  $T$  to 1, the shim gradually transitions from encoding large semantic changes to capturing finer semantic nuances. The attack can select a larger timestep to induce significant semantic alterations in copyrighted images or a smaller timestep to produce indistinguishable replicas that can evade invisible watermarks. Algorithm 1 illustrates our overall attack pipeline proposed in this work.

<sup>1</sup>The coefficient  $\zeta_t$  varies and is determined by different solvers. For example,  $\zeta_t = \left( \sqrt{1 - \alpha_t} - \sqrt{1 - \alpha_{t-1}} \right) \frac{\sqrt{\alpha_{t-1}}}{\sqrt{1 - \alpha_{t-1}}}$  in DDIM [44].

---

### Algorithm 1 The Attack Pipeline for Neural Plagiarism

---

```

1: Input:  $x^w$ 
2: Require: selected timesteps  $\mathcal{T}_{\text{select}}$ , perturbation function  $\Delta(\cdot)$ , learning rate  $\eta$ , coefficient  $\zeta_t^1$ , search depth  $K$  with total timesteps  $T$ , VAE encoder  $\mathcal{E}$  and decoder  $\mathcal{D}$ .
3:  $\hat{\mathbf{x}}_0 \leftarrow \mathcal{E}(x^w)$ 
4: for  $t = 1$  to  $T$  do
5:    $\hat{\mathbf{x}}_t \leftarrow \text{DPM Solver}(\hat{\mathbf{x}}_{t-1})$ 
6: end for
7: Initialize  $\mathbf{x}_K^* = \hat{\mathbf{x}}_K$  or  $\sqrt{\bar{\alpha}_K} \mathbf{x}_0 + \sqrt{1 - \bar{\alpha}_K} \epsilon$ 
8: for  $t = K$  to 1 do
9:   if  $t \in \mathcal{T}_{\text{select}}$  then  $\triangleright$  Enable gradient propagation
10:    Initialize  $\delta_t \leftarrow \mathbf{0}$ 
11:    while  $\delta_t$  not converged do
12:       $\mathbf{x}_{t-1}^* \leftarrow \mathbf{x}_t^* - \zeta_t \cdot \epsilon_\theta(\mathbf{x}_t^*, t, \mathbf{e}_\theta + \delta_t)$ 
13:       $\delta_t \leftarrow \delta_t - \eta \nabla \mathcal{L}(t, \delta_t, \mathbf{x}_{t-1}^*, \hat{\mathbf{x}}_{t-1})$ 
14:    end while
15:   else  $\triangleright$  Disable gradient propagation
16:      $\mathbf{x}_{t-1}^* \leftarrow \mathbf{x}_t^* - \zeta_t \cdot \epsilon_\theta(\mathbf{x}_t^*, t, \mathbf{e}_\theta)$ 
17:   end if
18: end for
19: Output:  $x^* \leftarrow \mathcal{D}(\mathbf{x}_0^*)$ 

```

---

## 6. Experiments

### 6.1. Setups

**Datasets.** We select MS-COCO to evaluate our attack performance as the several watermarking methods [13, 56] utilize MS-COCO for training or fine-tuning. We randomly sample images from the MS-COCO dataset [25] and crop them to  $512 \times 512$  resolution. Additionally, we generate  $512 \times 512$  images using corresponding prompts with Stable Diffusion (e.g., ‘‘stable-diffusion-2-1-base’’ [38]).

**Search Configuration.** By default, we adopt the Adam optimizer [23] with a learning rate of 0.01. To stabilize the optimization process, we utilize weight decay (i.e., L2 regularization, set to  $10^{-3}$ ) to balance the shims and apply gradient norm clipping (with a maximum norm of 1.0) to prevent exploding gradients. We use DPM solver [29] with a scheduler of 50 timesteps. For hyper-parameters, we set  $\gamma_1 = 10^5$ ,  $\gamma_2 = 0.1$  and  $\hat{\epsilon}_t = 10$  for every timestep.

### 6.2. Forgery Attack on Copyrighted Images

Forgery attacks aim to generate replicated images that bypass copyright protections. We investigate two scenarios: attacks on copyrighted images and invisible watermark removal. We compare our approach against two baseline regeneration attacks. Regen [59] adds noise at a specific timestep and then immediately denoises, while Rinse [3] repeats this process multiple times (e.g., twice). Notably, all experiments employ the same model architecture and

Method	Late start, noisy latent						Early start, inverse latent					
	BA ↓	ACC ↓	T1%F ↓	PSNR ↑	SSIM ↑	FID ↓	BA ↓	ACC ↓	T1%F ↓	PSNR ↑	SSIM ↑	FID ↑
<b>DwtDctSvd (32 bits)</b>												
Watermarked	1.00	1.00	1.00	38.33	0.99	3.54	1.00	1.00	1.00	39.48	0.99	3.02
Regen	0.64	0.15	0.00	26.21	0.75	36.48	0.63	0.14	0.00	25.51	0.80	21.36
Rinse	0.54	0.04	0.00	23.68	0.68	87.33	0.59	0.12	0.00	23.34	0.73	37.98
<b>Ours</b>	0.52	0.01	0.00	25.27	0.73	41.69	0.52	0.03	0.00	21.16	0.70	71.14
<b>RivaGAN (32 bits)</b>												
Watermarked	1.00	1.00	1.00	40.57	0.98	3.81	1.00	1.00	1.00	40.60	0.98	3.62
Regen	0.60	0.05	0.00	26.21	0.75	34.85	0.59	0.01	0.00	25.40	0.79	21.27
Rinse	0.52	0.01	0.00	23.74	0.68	82.72	0.53	0.01	0.00	23.42	0.73	36.98
<b>Ours</b>	0.56	0.02	0.00	25.29	0.73	40.80	0.52	0.00	0.00	21.15	0.70	71.14

Table 1. Watermark removal for invisible post-hoc watermarking on COCO images. A lower FID is preferred when removing invisible watermarks and a higher FID is preferred to encourage semantic changes for altering copyrighted images.

weights, without additional components such as extra image encoders or ControlNet adapters, differing only in the generation pipeline.

### 6.2.1. Invisible Watermark Removal

We use the benchmark [59] to evaluate our method on invisible watermark removal. Particularly, we employ performance metrics including: the changes in bit accuracy (BA), accuracy (ACC) defined as more than  $\frac{2}{3}$  bits correctly identified, and the True Positive Rate when False Positive Rate below 1% ( $T@1\%F$ ), which is commonly recommended by the benchmark [6, 59]; For image generation quality and semantic similarity, we measure Peak Signal-to-Noise Ratio (PSNR) [15], Structural Similarity Index (SSIM) [31] and Fréchet Inception Distance (FID) [19].

**Post-hoc Watermarking Methods:** we explore two common post-hoc watermarking methods, DctDwtSvd [17] and RivaGAN [56], which are applied on both real images and generated images using MS-COCO.

As in Algorithm 1, our attack starts at timestep  $K$  and backward step by step until reaching timestep 1. An early start indicates that we begin at a large timestep, while a late start corresponds to beginning at a smaller timestep.

- **Late start with noisy latent:** small perturbations are effective for removing invisible watermarks while preserving the original image quality. To achieve this, we begin our attack at later timestep ( $K = 140$ ) and insert shims at selected timesteps 100 and 60. For this setting, we use a noisy start defined as  $\mathbf{x}_K^* = \sqrt{\alpha_K} \mathbf{x}_0 + \sqrt{1 - \alpha_K} \epsilon$  since we observed that starting with inverse latent leads to limited semantic changes and is ineffective for invisible watermark removal. Consequently, although our approach shares the same starting latent as Regen [59], our approach works much better due to the perturbation shims of our method. As shown in Table 1 (left column), our method achieves significantly improved watermark removal performance, close to 50% bit accuracy, while

maintaining moderate PSNR, SSIM, and FID.

- **Early start with inverse latent:** large perturbations cause dramatic alterations to image features, which may remove the watermark in the image. We explore this settings with beginning time step  $K = 1000$  and insert shims at selected timesteps 600 and 200 to induce a large perturbation on attack images. As shown in Table 1 (right column), the detection bit accuracy also drops to nearly 50%, indicating successful watermark removal. However, this approach significantly alters the feature distribution, resulting in much higher FID scores compared to other settings. Notably, a high FID here does not necessarily imply that the attacked images are of low quality or noisy, as our method encourages meaningful semantic changes instead to random noise.

**Why these settings?** In Table 2, we visualize the pixel differences between the target images (watermarked images) and the attack images to illustrate the semantic changes induced by the shims. When we use the inverse latent as startup latent at a large timestep (early start), it induces significant semantic changes, for example, altering color of a bus, shape of traffic lights or the design of windows. In contrast, starting with the inverse latent at a small timestep (late start) produces minor and localized semantic changes, as major semantic changes have already been handled in previous timesteps. In this case, we use a noise latent to force the search for all detailed semantic changes, thereby improving the performance for invisible watermark removal (See Appendix for visualizations of all other cases.).

**Latent Watermarking Methods:** we also investigate two methods that apply watermarking in the latent space: Stable Signatures [13] and Tree-Ring [52]. Table 3 shows the results. It is clear that because the shims alter the latent variables, they generate alternative image latents that can bypass Stable Signatures, a watermarking method that fine-tunes the VAE decoder. However, our method is unable to remove the Tree-Ring watermark, as it injects a pattern on

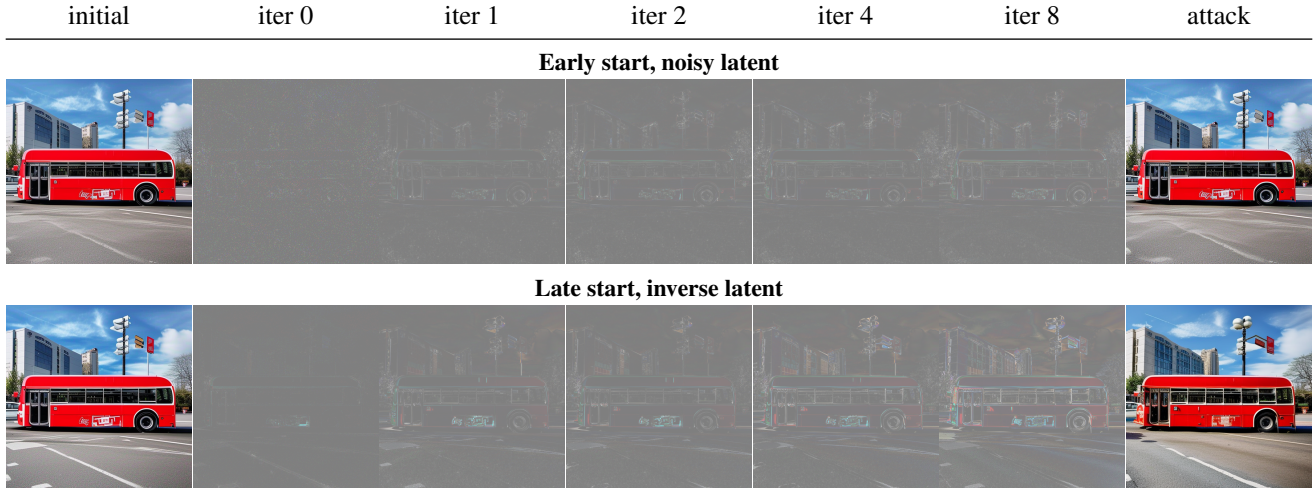


Table 2. The middle columns highlight the pixel differences between the initial image (leftmost) and the attack image (rightmost) during optimization. These illustrate how the latent gradually diverges from the anchor latent in a seamless and semantically meaningful manner.

latent variable in Fourier space using masking; even large shifts in the latent space do not significantly alter the local Fourier characteristics.

Method	T@1%F ↓	PSNR ↑	SSIM ↑	FID ↓
<b>Stable Signature</b>				
Watermarked	1.00	11.79	0.38	153.14
Regen	0.00	24.94	0.78	24.91
Rinse	0.00	22.96	0.72	46.85
<b>Ours</b>	0.00	24.08	0.80	43.83
<b>Tree-ring</b>				
Watermarked	1.00	12.99	0.49	122.20
Regen	1.00	26.79	0.81	22.73
Rinse	1.00	23.68	0.75	39.96
<b>Ours</b>	0.98	25.84	0.86	33.50

Table 3. Watermark removal for diffusion-based watermarking.

However, this result does not mean that Tree-Ring is practical for copyright protection. Tree-Ring suffers from ambiguity attacks. In particular, the optimal threshold chosen by the  $T@1\%F$  metric can create confusion among different watermark keys, causing images to be falsely classified as watermarked even when they were not watermarked with this key [8].

### 6.2.2. Copyrighted Images Replicas

We collect a set of online copyrighted images that include the common practices for copyright protection. The results are summarized in Table 4. To evaluate the degree of semantic modification, we apply shims on various timesteps.

It is clear that Regen [59] and Rinse [3] can partially remove copyright content. Despite of significant noise introduced, the resulting images remain similar enough to the

originals, which would very likely be disputed as clear plagiarism. In contrast, our method can easily generate replicas while bypassing the copyrights restriction. For example, Elsa’s iconic “sophisticated braided updo” hairstyle and “icy elegance layer skirt” are being replaced with short hair and suspender skirt, creating a blurring line for the Disney copyrighted anime. Additionally, we produce replicas for for Elon Musk, featured a thinner face with noticeable structural changes, which are uncommon in traditional AI deepfake. We also present Elon100, with 100 distinct replicas of Elon’s portrait, none of which can be definitively identified as him by a GPT arbiter. (See appendix for more details)

**Neural Plagiarism in Real-world:** attackers can choose different timesteps or shims within the proposed attack pipeline, generating a large amount of replicas using random seeds. When targeting copyrighted images that feature visible trademarks, signatures, or IPs, they can cherry-pick the best replicas to bypass the copyright restrictions. Besides, the pipeline accepts both prompt inputs and negative prompts, the final attacks can be even more potent in real-world scenarios.

### 6.3. Ambiguity Attacks

This is one of the most significant threat to copyright protection and has not received enough attention in the research community. We present two primary attack strategies:

- **Watermark Replacement:** In the case of RivaGAN, we remove the original watermark via our attack pipeline and subsequently inserting a new watermark  $w^*$ . This watermark replacement effectively nullifies the original copyright protection and thereby introduce copyright ambiguity with new watermark. As shown in Table 5, the new watermark  $w^*$  receives higher bit accuracy than the orig-

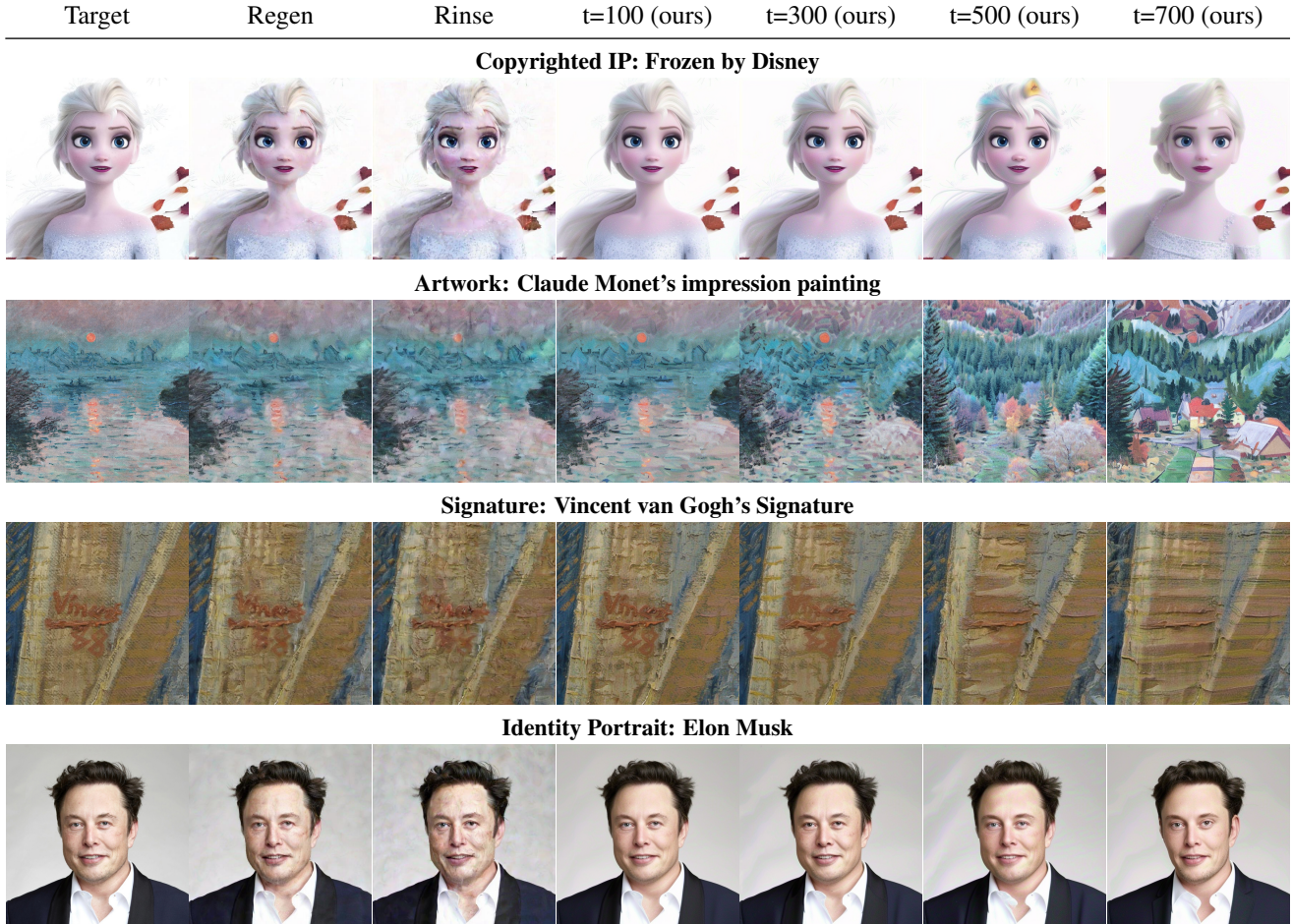


Table 4. Plagiarize copyrighted images.

inal one.

- **Co-existing Watermarks:** In the case of Tree-Ring, a latent watermark is injected into the inverse latent  $\mathbf{x}_T^*$ . Without precise knowledge of the channel containing the original watermark, the new watermark is embedded in an alternative channel, leading to the coexistence of both watermarks. From Table 5, both watermark receive high  $T@1\%F$ , creating ambiguity of data ownership.

Method	BA ( $w$ ) ↓	BA ( $w^*$ ) ↑	T@1%F ( $w$ ) ↓	T@1%F ( $w^*$ ) ↑
<b>RivaGAN (32 bits)</b>				
Watermarked	1.00	0.75	1.00	0.00
Attacked	0.75	1.00	0.00	1.00
<b>Tree-ring</b>				
Watermarked	-	-	1.00	0.00
Attacked	-	-	0.99	1.00

Table 5. Attack performance for ambiguity attacks. New watermark  $w^*$  can be successfully recovered on the attacked images, introducing ambiguity for data copyright.

## 7. Limitations and Future Work

Our method can remove most of watermark except for tree-ring; however, we can confuse the ownership detection successfully with alternative watermark key.

Some approaches could be used to enhance our attacks, including advanced image editing techniques [18], integration with plugins such as ControlNet adapters [27], image encoders [33], and negative prompts [4, 10]. We leave these as future work.

## 8. Conclusion

In this paper, we introduce a new threat, termed “neural plagiarism”, in which diffusion models plagiarize copyrighted images while bypassing protections like watermarking. We propose a universal attack pipeline that enables both forgery and ambiguity attacks, resulting in effective data plagiarism. With extensive experiments, our approach is effective to evade copyright protections ranging from visible copyrighted images to invisible watermarking.

**Acknowledgments:** This work was supported in part by NSF grants 1952792 and 2321572, and Google.

## References

- [1] Digital millennium copyright act (dmca). <https://www.copyright.gov/dmca/>, 1998. U.S. Copyright Office. Accessed: March 4, 2025. 2, 3
- [2] General data protection regulation (gdpr). <https://gdpr-info.eu/>, 2018. Accessed: March 4, 2025. 2
- [3] Bang An, Mucong Ding, Tahseen Rabbani, Aakriti Agrawal, Yuancheng Xu, Chenghao Deng, Sicheng Zhu, Abdirisak Mohamed, Yuxin Wen, Tom Goldstein, et al. Benchmarking the robustness of image watermarks. *ICML*, 2024. 2, 5, 7
- [4] Anonymous. Understanding the impact of negative prompts: When and how do they take effect?, 2024. arXiv preprint. 8
- [5] Nicholas Carlini, Florian Tramer, Eric Wallace, Matthew Jagielski, Ariel Herbert-Voss, Katherine Lee, Adam Roberts, Tom Brown, Dawn Song, Ulfar Erlingsson, et al. Extracting training data from large language models. In *30th USENIX Security Symposium (USENIX Security 21)*, pages 2633–2650, 2021. 1
- [6] Nicholas Carlini, Steve Chien, Milad Nasr, Shuang Song, Andreas Terzis, and Florian Tramer. Membership inference attacks from first principles. In *2022 IEEE symposium on security and privacy (SP)*, pages 1897–1914. IEEE, 2022. 6
- [7] Nicolas Carlini, Jamie Hayes, Milad Nasr, Matthew Jagielski, Vikash Sehwal, Florian Tramer, Borja Balle, Daphne Ippolito, and Eric Wallace. Extracting training data from diffusion models. In *32nd USENIX Security Symposium (USENIX Security 23)*, pages 5253–5270, 2023. 1
- [8] Hai Ci, Pei Yang, Yiren Song, and Mike Zheng Shou. Ringid: Rethinking tree-ring watermarking for enhanced multi-key identification. *arXiv preprint arXiv:2404.14055*, 2024. 7
- [9] Hai Ci, Pei Yang, Yiren Song, and Mike Zheng Shou. Ringid: Rethinking tree-ring watermarking for enhanced multi-key identification. In *European Conference on Computer Vision*, pages 338–354. Springer, 2025. 2
- [10] Stable Diffusion. 100 negative prompts everyone are using. <https://medium.com/stablediffusion/100-negative-prompts-everyone-are-using-c71d0ba33980>, 2022. Accessed: 2025-03-06. 8
- [11] Lixin Fan, Kam Woh Ng, and Chee Seng Chan. Rethinking deep neural network ownership verification: Embedding passports to defeat ambiguity attacks. *Advances in neural information processing systems*, 32, 2019. 3
- [12] Pierre Fernandez, Alexandre Sablayrolles, Teddy Furon, Hervé Jégou, and Matthijs Douze. Watermarking images in self-supervised latent spaces. In *ICASSP 2022-2022 IEEE International Conference on Acoustics, Speech and Signal Processing (ICASSP)*, pages 3054–3058. IEEE, 2022. 2
- [13] Pierre Fernandez, Guillaume Couairon, Hervé Jégou, Matthijs Douze, and Teddy Furon. The stable signature: Rooting watermarks in latent diffusion models. In *Proceedings of the IEEE/CVF International Conference on Computer Vision*, pages 22466–22477, 2023. 2, 5, 6
- [14] Ohad Fried, Ayush Tewari, Michael Zollhöfer, Adam Finkelstein, Eli Shechtman, Dan B Goldman, Kyle Genova, Zeyu Jin, Christian Theobalt, and Maneesh Agrawala. Text-based editing of talking-head video. *ACM Transactions on Graphics (TOG)*, 38(4):1–14, 2019. 2
- [15] Rafael C. Gonzalez and Richard E. Woods. *Digital Image Processing*. Prentice Hall, Upper Saddle River, NJ, 2nd edition, 2002. 6
- [16] Ian Goodfellow, Jean Pouget-Abadie, Mehdi Mirza, Bing Xu, David Warde-Farley, Sherjil Ozair, Aaron Courville, and Yoshua Bengio. Generative adversarial nets. In *Advances in Neural Information Processing Systems (NIPS)*, pages 2672–2680, 2014. 2
- [17] Mohamed Hamidi, Mohamed El Haziti, Hocine Cherifi, and Mohammed El Hassouni. A hybrid robust image watermarking method based on dwt-dct and sift for copyright protection. *Journal of Imaging*, 7(10):218, 2021. 2, 6
- [18] Amir Hertz, Ron Mokady, Jay Tenenbaum, Kfir Aberman, Yael Pritch, and Daniel Cohen-Or. Prompt-to-prompt image editing with cross attention control. *arXiv preprint arXiv:2208.01626*, 2022. 4, 8
- [19] Martin Heusel, Hubert Ramsauer, Thomas Unterthiner, Bernhard Nessler, and Sepp Hochreiter. Gans trained by a two time-scale update rule converge to a local nash equilibrium. In *Advances in Neural Information Processing Systems*, 2017. 6
- [20] Jonathan Ho, Ajay Jain, and Pieter Abbeel. Denoising diffusion probabilistic models. *Advances in neural information processing systems*, 33:6840–6851, 2020. 2, 3
- [21] Seongmin Hong, Kyeonghyun Lee, Suh Yoon Jeon, Hyewon Bae, and Se Young Chun. On exact inversion of dpm-solvers. In *Proceedings of the IEEE/CVF Conference on Computer Vision and Pattern Recognition*, pages 7069–7078, 2024. 3
- [22] Zhengyuan Jiang, Jinghuai Zhang, and Neil Zhenqiang Gong. Evading watermark based detection of ai-generated content. In *Proceedings of the 2023 ACM SIGSAC Conference on Computer and Communications Security*, pages 1168–1181, 2023. 2
- [23] Diederik P. Kingma and Jimmy Ba. Adam: A method for stochastic optimization. In *International Conference on Learning Representations (ICLR)*, 2015. 5
- [24] Diederik P Kingma, Max Welling, et al. Auto-encoding variational bayes, 2013. 3
- [25] Tsung-Yi Lin, Michael Maire, Serge Belongie, James Hays, Pietro Perona, Deva Ramanan, Piotr Dollár, and C Lawrence Zitnick. Microsoft coco: Common objects in context. In *Computer Vision—ECCV 2014: 13th European Conference, Zurich, Switzerland, September 6–12, 2014, Proceedings, Part V 13*, pages 740–755. Springer, 2014. 5
- [26] Chi Liu, Huajie Chen, Tianqing Zhu, Jun Zhang, and Wanlei Zhou. Making deepfakes more spurious: evading deep face forgery detection via trace removal attack. *IEEE Transactions on Dependable and Secure Computing*, 20(6):5182–5196, 2023. 2
- [27] Yepeng Liu, Yiren Song, Hai Ci, Yu Zhang, Haofan Wang, Mike Zheng Shou, and Yuheng Bu. Image watermarks are removable using controllable regeneration from clean noise. *arXiv preprint arXiv:2410.05470*, 2024. 2, 8

- [28] Yepeng Liu, Yiren Song, Hai Ci, Yu Zhang, Haofan Wang, Mike Zheng Shou, and Yuheng Bu. Image watermarks are removable using controllable regeneration from clean noise. In *The Thirteenth International Conference on Learning Representations*, 2025. 2
- [29] Cheng Lu, Yuhao Zhou, Fan Bao, Jianfei Chen, Chongxuan Li, and Jun Zhu. Dpm-solver: A fast ode solver for diffusion probabilistic model sampling in around 10 steps. *Advances in Neural Information Processing Systems*, 35:5775–5787, 2022. 3, 4, 5
- [30] KA Navas, Mathews Cheriyan Ajay, M Lekshmi, Tampy S Archana, and M Sasikumar. Dwt-dct-svd based watermarking. In *2008 3rd international conference on communication systems software and middleware and workshops (COM-SWARE'08)*, pages 271–274. IEEE, 2008. 2
- [31] Peter Ndajah, Hisakazu Kikuchi, Masahiro Yukawa, Hide-nori Watanabe, and Shogo Muramatsu. Ssim image quality metric for denoised images. In *Proc. 3rd WSEAS Int. Conf. on Visualization, Imaging and Simulation*, pages 53–58, 2010. 6
- [32] Alex Nichol, Prafulla Dhariwal, Aditya Ramesh, Pranav Shyam, Pamela Mishkin, Bob McGrew, Ilya Sutskever, and Mark Chen. Glide: Towards photorealistic image generation and editing with text-guided diffusion models. *arXiv preprint arXiv:2112.10741*, 2021. 5
- [33] Maxime Oquab, Timothée Darcet, Théo Moutakanni, Huy Vo, Marc Szafraniec, Vasil Khalidov, Pierre Fernandez, Daniel Haziza, Francisco Massa, Alaaeldin El-Nouby, et al. Dinov2: Learning robust visual features without supervision. *arXiv preprint arXiv:2304.07193*, 2023. 2, 8
- [34] William Peebles and Saining Xie. Scalable diffusion models with transformers. In *Proceedings of the IEEE/CVF international conference on computer vision*, pages 4195–4205, 2023. 2, 3
- [35] Alec Radford, Jong Wook Kim, Chris Hallacy, Aditya Ramesh, Gabriel Goh, Sandhini Agarwal, Girish Sastry, Amanda Askell, Pamela Mishkin, Jack Clark, et al. Learning transferable visual models from natural language supervision. In *International conference on machine learning*, pages 8748–8763. PMLR, 2021. 5
- [36] Aditya Ramesh, Mikhail Pavlov, Gabriel Goh, Scott Gray, Chelsea Voss, Alec Radford, Mark Chen, and Ilya Sutskever. Zero-shot text-to-image generation. *arXiv preprint arXiv:2102.12092*, 2021. 1
- [37] Aditya Ramesh, Prafulla Dhariwal, Alex Nichol, Casey Chu, and Mark Chen. Hierarchical text-conditional image generation with clip latents. *arXiv preprint arXiv:2204.06125*, 2022. 1
- [38] Robin Rombach, Andreas Blattmann, Dominik Lorenz, Patrick Esser, and Björn Ommer. High-resolution image synthesis with latent diffusion models. In *Proceedings of the IEEE/CVF Conference on Computer Vision and Pattern Recognition (CVPR)*, pages 10684–10695, 2022. 4, 5
- [39] Robin Rombach, Andreas Blattmann, Dominik Lorenz, Patrick Esser, and Björn Ommer. High-resolution image synthesis with latent diffusion models. In *Proceedings of the IEEE/CVF conference on computer vision and pattern recognition*, pages 10684–10695, 2022. 1, 2, 3
- [40] Olaf Ronneberger, Philipp Fischer, and Thomas Brox. U-net: Convolutional networks for biomedical image segmentation. In *Medical Image Computing and Computer-Assisted Intervention (MICCAI)*, pages 234–241. Springer, 2015. 3
- [41] Mehrdad Saberi, Vinu Sankar Sadasivan, Keivan Rezaei, Aounon Kumar, Atoosa Chegini, Wenxiao Wang, and Soheil Feizi. Robustness of ai-image detectors: Fundamental limits and practical attacks. *arXiv preprint arXiv:2310.00076*, 2023. 2
- [42] Chitwan Saharia, William Chan, Saurabh Saxena, Lala Li, Jay Whang, Emily Denton, Suman Kundu, and Mohammad Norouzi. Photorealistic text-to-image diffusion models with deep language understanding, 2022. Imagen: Photorealistic Text-to-Image Diffusion Models. 1
- [43] Jascha Sohl-Dickstein, Eric Weiss, Niru Maheswaranathan, and Surya Ganguli. Deep unsupervised learning using nonequilibrium thermodynamics. In *International conference on machine learning*, pages 2256–2265. PMLR, 2015. 2, 3
- [44] Jiaming Song, Chenlin Meng, and Stefano Ermon. Denoising diffusion implicit models. *arXiv preprint arXiv:2010.02502*, 2020. 2, 3, 5
- [45] Supasorn Suwajanakorn, Steven M Seitz, and Ira Kemelmacher-Shlizerman. Synthesizing obama: learning lip sync from audio. *ACM Transactions on Graphics (ToG)*, 36(4):1–13, 2017. 2
- [46] Matthew Tancik, Ben Mildenhall, and Ren Ng. Stegastamp: Invisible hyperlinks in physical photographs. In *Proceedings of the IEEE/CVF conference on computer vision and pattern recognition*, pages 2117–2126, 2020. 2, 3
- [47] Justus Thies, Michael Zollhofer, Marc Stamminger, Christian Theobalt, and Matthias Nießner. Face2face: Real-time face capture and reenactment of rgb videos. In *Proceedings of the IEEE conference on computer vision and pattern recognition*, pages 2387–2395, 2016. 2
- [48] United States Patent and Trademark Office. Trademark law. <https://www.uspto.gov/sites/default/files/documents/tmlaw.pdf>, n.d. 2, 3
- [49] Ashish Vaswani, Noam Shazeer, Niki Parmar, Jakob Uszkoreit, Llion Jones, Aidan N Gomez, Łukasz Kaiser, and Illia Polosukhin. Attention is all you need. *Advances in neural information processing systems*, 30, 2017. 4
- [50] Bram Wallace, Akash Gokul, and Nikhil Naik. Edict: Exact diffusion inversion via coupled transformations. In *Proceedings of the IEEE/CVF Conference on Computer Vision and Pattern Recognition*, pages 22532–22541, 2023. 3
- [51] Ruo Chen Wang, Ting Liu, Cho-Jui Hsieh, and Boqing Gong. On discrete prompt optimization for diffusion models. In *International Conference on Machine Learning (ICML)*, 2024. 4
- [52] Yuxin Wen, John Kirchenbauer, Jonas Geiping, and Tom Goldstein. Tree-rings watermarks: Invisible fingerprints for diffusion images. In *Advances in Neural Information Processing Systems*, pages 58047–58063. Curran Associates, Inc., 2023. 2, 3, 4, 6
- [53] Zijin Yang, Kai Zeng, Kejiang Chen, Han Fang, Weiming Zhang, and Nenghai Yu. Gaussian shading: Provable performance-lossless image watermarking for diffusion

- models. In *Proceedings of the IEEE/CVF Conference on Computer Vision and Pattern Recognition*, pages 12162–12171, 2024. [2](#), [4](#)
- [54] Zihan Yuan, Li Li, Zichi Wang, and Xinpeng Zhang. Ambiguity attack against text-to-image diffusion model watermarking. *Signal Processing*, 221:109509, 2024. [3](#)
- [55] Jie Zhang, Dongdong Chen, Jing Liao, Weiming Zhang, Gang Hua, and Nenghai Yu. Passport-aware normalization for deep model protection. *Advances in Neural Information Processing Systems*, 33:22619–22628, 2020. [3](#)
- [56] Kevin Alex Zhang, Lei Xu, Alfredo Cuesta-Infante, and Kalyan Veeramachaneni. Robust invisible video watermarking with attention. 2019. [2](#), [5](#), [6](#)
- [57] Lvmin Zhang, Anyi Rao, and Maneesh Agrawala. Adding conditional control to text-to-image diffusion models, 2023. [1](#), [2](#)
- [58] Richard Zhang, Phillip Isola, Alexei A Efros, Eli Shechtman, and Oliver Wang. The unreasonable effectiveness of deep features as a perceptual metric. In *Proceedings of the IEEE conference on computer vision and pattern recognition*, pages 586–595, 2018. [3](#)
- [59] Xuandong Zhao, Kexun Zhang, Zihao Su, Saastha Vasan, Ilya Grishchenko, Christopher Kruegel, Giovanni Vigna, Yu-Xiang Wang, and Lei Li. Invisible image watermarks are provably removable using generative ai. *arXiv preprint arXiv:2306.01953*, 2023. [2](#), [3](#), [5](#), [6](#), [7](#)
- [60] J Zhu. Hidden: hiding data with deep networks. *arXiv preprint arXiv:1807.09937*, 2018. [2](#), [3](#)